

Demonstration of Interference of Polarized Light with a Wedge Depolarizer

Shengli Pu

College of Science, University of Shanghai for Science and Technology, Shanghai 200093, China

Email: shlpu@usst.edu.cn

(Submitted June 2010)

Abstract

A simple experimental configuration for the demonstration of interference of polarized light is presented in this paper. Using the wedge depolarizer, a nice and direct demonstration of interference of polarized light is realized, which would help to impress on students the phenomena of interference of polarized light intuitively. Moreover, this experiment can be easily implemented in the undergraduate/postgraduate optics laboratory because of its simple setup, and there is no need for expensive equipment.

1. Introduction

For some applications, the polarization-sensitive devices may cause considerable errors or degrade the performance of the systems when the incident light is not completely unpolarized. For example, the polarization-sensitive detector will result in errors and noise in the optical sensing and spectrum measurement systems; the polarization-dependent effects in optical fiber communication system may reduce its performance. Therefore, completely unpolarized light is desirable for some cases. Under this requirement, the term depolarization and the corresponding device depolarizer (which couple the polarized light into the unpolarized one) occur. As we know, it is easy to get the polarized light via unpolarized one (e.g. using a polarizer). Contrarily, it is more or less difficult to depolarize the polarized light. Thanks to the development of depolarizers, the equivalently unpolarized light can be realized at present. Besides these, I have casually found that the commercially available wedge-type depolarizer can be employed to demonstrate the interference of polarized light easily and nicely in our optics laboratory. The underlying physical principle is fundamental for undergraduate/postgraduate students, but the

interference patterns are splendid, which may be impressive for students. This article first gives a brief introduction to the present depolarizers and the theory of interference of polarized light. Then the wedge depolarizer is chosen to demonstrate the interference of polarized light. With the wedge depolarizer, versatile and obvious interference patterns are observed experimentally.

2. Depolarizers and interference of polarized light

Strictly speaking, the present depolarizers in fact are wavelength-dependent^{1,2} or temporal³/spatial⁴ pseudo-depolarizers according to the mechanisms of depolarization. The transmitted light of the currently used depolarizers are not genuine unpolarized light, but compose of much light with various wavelength-dependent states of polarization or various states of polarization temporally/spatially. The collective effects of the transmitted light equal those of the unpolarized light. So the current depolarizers are pseudo-depolarizers in nature. According to their structures, the typical pseudodepolarizers can be classified into two kinds: Lyot depolarizers and wedge depolarizers. The Lyot depolarizer consists of two crystalline plates of thickness ratio 2:1,

whose optical axes lie in the planes of the plates and are oriented at 45° to one another.^{5,6} It creates various degrees of elliptical polarization as a function of wavelength, therefore it is a wavelength-dependent depolarizer and not suitable for the monochromatic light application. The wedge depolarizer consists of a wedge birefringent crystal, whose optical axis lies in the plane of the wedge and usually at 45° to the input polarization for the maximum performance of depolarization. Consequently, it is sensitive to the input polarization direction. Fig. 1 schematically draws the structure of the wedge depolarizer. Because of the varying thickness of crystal at different loci of the wedge, the phase retardation between the

$$I = I_0 (\cos^2 \alpha \cos^2 \beta + \sin^2 \alpha \sin^2 \beta + 2 \cos \alpha \cos \beta \sin \alpha \sin \beta \cos \delta)$$

$$= I_0 \cos^2(\alpha + \beta) + \frac{I_0}{2} \sin 2\alpha \sin 2\beta (1 + \cos \delta), \quad (1)$$

where α / β are the included angles between the transmission axes of the polarizer/analyzer and the electric vector of the extraordinary (or ordinary) light in the retardation sheet (see Fig. 2), δ is the phase retardation of the transmitted light, which depends on the relative orientation of the linearly polarized light and the parameters of the retardation sheet (also depends on wavelength for polychromatic light). By changing α , β or δ , the intensity or patterns on the screen can be changed according to Eq. (1). This will demonstrate the interference of polarized light.

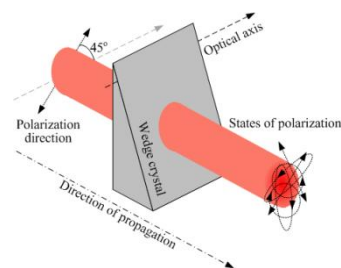


Figure 1. Schematic structure of the wedge depolarizer.

ordinary and extraordinary light (depending on the thickness) is diversified. This results in the transmitted light composed of multiple degrees of elliptical polarization.

The typical experimental setup for investigating the interference of polarized light is shown in Fig. 2. A linearly polarized incident light impinges on the retardation sheet, and then passes through an analyzer. The interference of polarized light can be observed on the screen. If the intensity of the linearly polarized incident light is I_0 , the intensity of the transmitted light on the screen is given as follows (according to Malus's law),

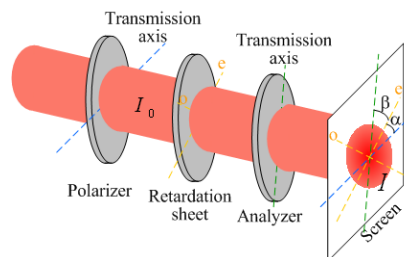


Figure 2. Experimental setup for investigating the interference of polarized light.

3. Experiment

As the wedge depolarizer is a birefringent crystal with varying thickness and commercially available, it is a good candidate device for demonstrating the interference of polarized light. When the retardation sheet in Fig. 2 is replaced with a wedge depolarizer, wonderful interference patterns of the polarized light can be observed. From Eq. (1), the following results are easily obtained and the corresponding experimental

interference patterns are photographed by a digital CCD camera and shown in Figs. 3-6, respectively. The spatial configurations of the optical components are schematically depicted in the right panels of the corresponding figures.

When $\alpha = 0^\circ$ and $\beta = 90^\circ$ (or $\alpha = 90^\circ$ and $\beta = 0^\circ$), $I = 0$, viz dark field happens on the screen, which can be seen in Fig. 3.

When $\alpha = 0^\circ$ (or 90°), $I = I_0 \cos^2 \beta$ (or $I_0 \sin^2 \beta$), namely the intensity on the screen are uniform spatially and only depend on the value of β [see Figs. 4(a) and (b) for $\beta = 30^\circ$ and 45° , respectively]. From Fig. 4, the intensities of the interference patterns are almost uniform everywhere. The brightness in Fig. 4(b) is slightly weaker than that in Fig. 4(a), which is due to $\cos^2 45^\circ < \cos^2 30^\circ$.

When $\beta = 0^\circ$ (or 90°), $I = I_0 \cos^2 \alpha$ (or $I_0 \sin^2 \alpha$). This is very similar to Case 2 (Fig. 4) and the experimental interference patterns are not shown here in.

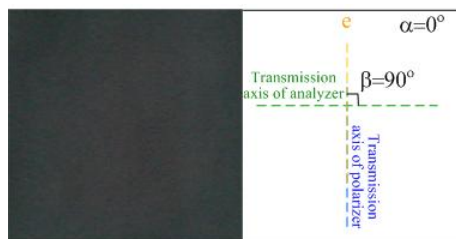


Figure 3. Interference pattern for $\alpha = 0^\circ$ and $\beta = 90^\circ$. Dark field happens on the screen.

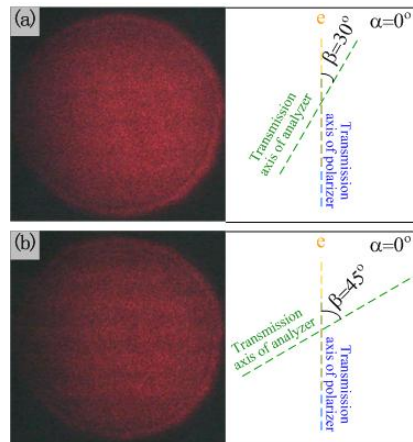


Figure 4. Interference patterns for $\alpha = 0^\circ$, (a) $\beta = 30^\circ$ and (b) $\beta = 45^\circ$. Intensities of the interference patterns are almost uniform spatially.

For the above cases, the second term on the right hand side of Eq. (1) is always equal to zero. On the other hand, it will have various values when $\alpha \neq 0^\circ/90^\circ$ and $\beta \neq 0^\circ/90^\circ$. For the fixed values of α and β , the intensity on the screen only depends on the phase retardation δ , i.e. the thickness of the retardation sheet (considering monochromatic light). As the wedge depolarizer has a varying thickness spatially, the spatial distribution of the intensity on the screen I must be periodic like the variation of the thickness of the depolarizer. This periodic distribution of intensity constitutes the interference fringes and their orientation coincides with the direction of the axis of the wedge depolarizer (viz the isopachous lines of the wedge). Under this situation, the first term on the right hand side of Eq. (1) influences the visibility of the fringe patterns. And then the phenomena of the interference can be classified into two cases (maintaining $\alpha \neq 0^\circ/90^\circ$ and $\beta \neq 0^\circ/90^\circ$).

When $\alpha + \beta = 90^\circ$ (or 270°), the intensity of the dark regions of the interference fringe patterns equals zero [because the first term on the right hand side of Eq. (1) equals zero], which results in

the maximum visibility of the fringe patterns. (a) Maximum intensity of the bright fringe happens for $\alpha = \beta = 45^\circ$ [see Fig. 5(a)]. (b) Reduced intensity of the bright fringe happens for other values of α and β , for instance, $\alpha = 30^\circ$ and $\beta = 60^\circ$ [see Fig. 5(b)]. From Fig. 5, it is revealed that there is almost no light in the dark areas of the interference patterns. Comparing with that in Fig. 5(a) ($\alpha = \beta = 45^\circ$), the reduced intensity of the bright fringe in Fig. 5(b) ($\alpha = 30^\circ$ and $\beta = 60^\circ$) is not obvious, but can be noticed by careful observation of the two photographs.

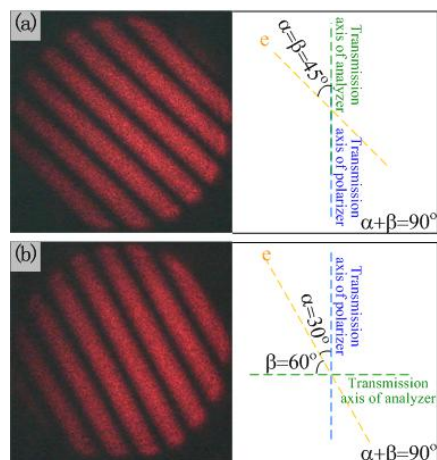


Figure 5. Interference patterns for (a) $\alpha = \beta = 45^\circ$ and (b) $\alpha = 30^\circ$, $\beta = 60^\circ$ ($\alpha + \beta = 90^\circ$ for both situations). Maximum visibility of the fringe patterns happens.

When $\alpha + \beta \neq 90^\circ$ (or 270°), the visibility of the patterns will be degraded contributed to the nonzero value of the first term on the right hand side of Eq. (1). Figs. 6(a) and (b) display the experimental interference patterns for $\alpha = \beta = 30^\circ$ and $\alpha = 30^\circ$ and $\beta = 45^\circ$, respectively. It is apparent that the intensity of the dark regions of the interference patterns is nonzero, which is different from Fig. 5. Consequently, the visibility

of the interference patterns weakened to some extent compared with those in Fig. 5.

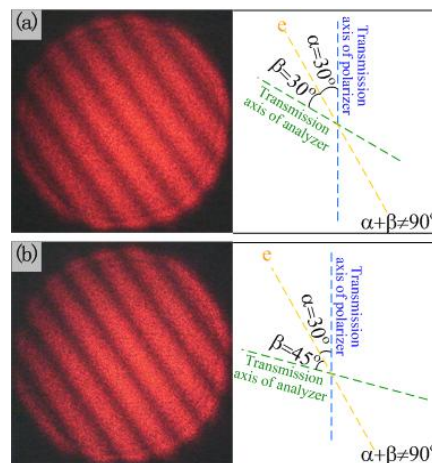


Figure 6. Interference patterns for (a) $\alpha = \beta = 30^\circ$ and (b) $\alpha = 30^\circ$, $\beta = 45^\circ$ ($\alpha + \beta \neq 90^\circ$ for both situations). The visibility of the fringe patterns is degraded relatively.

Figs. 5 and 6 show that the orientation of the interference fringes always coincides with the optical axis of the wedge depolarizer and is independent of the positions of the transmission axes of the polarizer and analyzer. This confirms the forementioned theoretical analysis. Further experiments have readily found that the orientation of the interference fringes can be changed by rotating the wedge depolarizer about the propagation direction of the light beam, i.e. its optical axis. In short, the above experimental results have a good agreement with the theoretical predictions based on Eq. (1).

4. Conclusions

Experiments indicate that the commercially available wedge depolarizer is a useful tool for the easy and impressive demonstration of the interference of polarized light. It may help students better understand the nature of polarized

light. In addition, the method presented in this paper is cost-effective to equip the corresponding undergraduate/postgraduate optics laboratory with wedge depolarizers to investigate the interference of polarized light.

Acknowledgements

This work was funded by the Research Fund for Selecting and Training Excellent Young Teachers in Universities of Shanghai, Shanghai Municipal Education Commission; and partially supported by the National Natural Science Foundation of China under Grant No. 10704048. The author

thanks Professor J. Shen in our department for his enlightening discussions.

References :

1. S.-L Lu, and A. P. Loeber, J. Opt. Soc. Am. **65**, 248 (1975).
2. A. A. Kokhanovsky, Am. J. Phys. **72**, 258 (2004).
3. I. Yoon, B. Lee, and S.-J. Park, J. Lightwave Technol. **25**, 1848 (2007).
4. D. Zhang *et al.*, Opt. Eng. **46**, 070504 (2007).
5. A. P. Loeber, J. Opt. Soc. Am. **72**, 650 (1982).
6. P. H. Richter, J. Opt. Soc. Am. **69**, 460 (1979)